



**HAL**  
open science

## When insect pests build their own thermal niche: The hot nest of the pine processionary moth

Laura Poitou, Christelle Robinet, Christelle Suppo, Jérôme Rousselet,  
Mathieu Laparie, Sylvain Pincebourde

### ► To cite this version:

Laura Poitou, Christelle Robinet, Christelle Suppo, Jérôme Rousselet, Mathieu Laparie, et al.. When insect pests build their own thermal niche: The hot nest of the pine processionary moth. *Journal of Thermal Biology*, 2021, 98, pp.102947. 10.1016/j.jtherbio.2021.102947 . hal-03320822

**HAL Id: hal-03320822**

**<https://hal.science/hal-03320822v1>**

Submitted on 5 Oct 2021

**HAL** is a multi-disciplinary open access archive for the deposit and dissemination of scientific research documents, whether they are published or not. The documents may come from teaching and research institutions in France or abroad, or from public or private research centers.

L'archive ouverte pluridisciplinaire **HAL**, est destinée au dépôt et à la diffusion de documents scientifiques de niveau recherche, publiés ou non, émanant des établissements d'enseignement et de recherche français ou étrangers, des laboratoires publics ou privés.

1  
2  
3  
4  
5  
6  
7  
8  
9  
10  
11  
12  
13  
14  
15  
16  
17  
18  
19  
20  
21  
22  
23  
24  
25  
26  
27

**When insect pests build their own thermal niche: the hot nest of the pine processionary moth**

Laura Poitou<sup>1</sup>, Christelle Robinet<sup>1</sup>, Christelle Suppo<sup>2</sup>, Jérôme Rousselet<sup>1</sup>, Mathieu Laparie<sup>1</sup>,  
Sylvain Pincebourde<sup>2\*</sup>

<sup>1</sup>INRAE, URZF, 45075, Orléans, France

<sup>2</sup>Institut de Recherche sur la Biologie de l’Insecte, UMR 7261, CNRS - Université de Tours,  
37200 Tours, France.

**\*Corresponding author:** Sylvain Pincebourde (sylvain.pincebourde@univ-tours.fr)

Journal: Journal of Thermal Biology

Type of paper: Original paper

28 **Abstract**

29 Temperature strongly drives physiological and ecological processes in ectotherms. While many  
30 species rely on behavioural thermoregulation to avoid thermal extremes, others build structures  
31 (nests) that confer a shelter against climate variability and extremes. However, the microclimate  
32 inside nests remains unknown for most insects. We investigated the thermal environment inside  
33 the nest of a temperate winter-developing insect species, the pine processionary moth (PPM),  
34 *Thaumetopoea pityocampa*. Gregarious larvae collectively build a silken nest at the beginning  
35 of the cold season. We tested the hypothesis that it provides a warmer microenvironment to  
36 larvae. First, we monitored temperature inside different types of nests varying in the number of  
37 larvae inside. Overall, nest temperature was positively correlated to global radiation and air  
38 temperature. At noon, when global radiation was maximal, nest temperature exceeded air  
39 temperature by up to 11.2-16.5°C depending on nest type. In addition, thermal gradients of  
40 amplitude from 6.85 to 15.5°C were observed within nests, the upper part being the warmest.  
41 Second, we developed a biophysical model to predict temperature inside PPM nests based on  
42 heat transfer equations and to explain this important temperature excess. A simple model  
43 version accurately predicted experimental measurements, confirming that nest temperature is  
44 driven mainly by radiation load. Finally, the model showed that nest temperature increases at  
45 the same rate as air temperature change. We conclude that some pest insects already live in  
46 warm microclimates by building their own sheltering nest. This effect should be considered  
47 when studying the impact of climate change on phenology and distribution.

48

49 **Keywords:** Microclimate, pine processionary moth, biophysical ecology, heat gain, nest,  
50 thermal niche.

51

52

## 53        **1. Introduction**

54            Temperature is the most impactful environmental variable for organisms since it drives  
55 virtually all biochemical processes and physiological rates (Walther et al., 2002). Temperature  
56 influences ectotherms at all levels from their physiology (Chown and Nicolson, 2004) to their  
57 geographic distributions (Menéndez, 2007). The vast majority of studies attempting to relate  
58 temperature and ecological or physiological processes in ectotherms uses ambient air or  
59 atmospheric temperature, often taken at relatively coarse spatial scale, as a proxy of the  
60 temperature experienced by organisms in their microhabitat (Kearney and Porter, 2009; Potter  
61 et al., 2013). Small ectotherms like insects, however, live in thermal habitats that can deviate  
62 substantially from ambient air temperature and that can vary according to patterns that differ  
63 from environmental fluctuations (Pincebourde et al., 2016; Pincebourde and Woods, 2020). For  
64 example, tropical ants can be confined to superheated plant surfaces in the canopy, thereby  
65 experiencing temperatures up to 25°C above ambient air temperature (Kaspari et al., 2015).  
66 Temperate aphids or spider mites also experience temperatures up to 20°C above ambient  
67 temperature at the surface of leaves exposed to solar radiation (Caillon et al., 2014; Saudreau  
68 et al., 2017; Cahon et al., 2018). Therefore, the temperature of the microclimate should be  
69 considered to better comprehend the global response of insects to environmental temperature  
70 variations. Yet, the microclimatic temperature to which most animals and plants are exposed  
71 remains to be quantified (Lembrechts et al., 2020; Pincebourde and Sallé, 2020; Pincebourde  
72 and Woods, 2020).

73            Some species build structures for diverse functions during part or all of their life cycle.  
74 These animal constructions can generate novel microclimates with specific temperature  
75 patterns that ameliorate their survival or fitness (concept of extended phenotype; (Dawkins,  
76 1982)). A well-known example is the large termite mound in Africa, which greatly buffers the  
77 extreme environmental temperatures thereby improving survival in otherwise quite challenging  
78 thermal environments (Joseph et al., 2016). Many other insects build or induce more cryptic  
79 structures (Hansell, 2007) such as leaf mines, plant galls, or tunnels across the wood. Despite  
80 their small size, the microclimate temperature within these structures can deviate strongly from  
81 ambient air temperature (Pincebourde and Casas, 2016). For example, the temperature inside  
82 leaf mines can be up to ~15°C warmer than ambient air (Pincebourde and Casas, 2006, 2015).  
83 The nest of social insects including bees and wasps also generates particular thermal  
84 environments, mostly due to the ability of social insects to thermoregulate the atmosphere inside  
85 the nest (Hozumi et al., 2010; Stabentheiner et al., 2010). Finally, gregarious insects complete

86 part of their larval development by building nests often made of silk produced by individuals.  
87 This is the case of some Lepidopteran species whose communal nests generate microclimate  
88 temperatures that can deviate by up to 2-5°C from ambient air (Knapp and Casey, 1986; Ruf  
89 and Fiedler, 2000; Fitzgerald et al., 2012). In all those structures, heat is exchanged with the  
90 environment through i) conduction across the boundary layer of the structure, ii) convection in  
91 the ambient air, iii) absorption and emission of radiative energy, and iv) possibly also during  
92 evapotranspiration (Gates and Schmerl, 1980; Monteith and Reifsnnyder, 2008). The relative  
93 rate of heat exchanged via those four processes depends on environmental properties like air  
94 temperature, wind speed and amount of solar radiation received, but also on the structure  
95 properties like its size, shape and color. For most insect structures, the convection is the main  
96 source of heat losses, whereas solar radiation constitutes the main heat source (May, 1979).  
97 Nevertheless, these mechanisms are rarely considered to characterize the microclimate of  
98 structures developed by insect pests.

99 Insect constructions not only generate novel microclimates but also sometimes provide  
100 insects with heterogeneous micro-environments inside which they can thermoregulate.  
101 Behavioural thermoregulation is an important process that allows insects to stabilize their body  
102 temperature or at least to buffer extremes (May, 1979; Woods et al., 2015). Both the architecture  
103 and the position within the structure are important components of this process. For example,  
104 the codling moth *Cydia pomonella*, develops within apple fruit (although this is not a structure  
105 built by the insect) and, under normal conditions, they select the warmer apple hemisphere, *i.e.*  
106 the one that receives solar radiation (Kührt et al., 2005). The fall webworm *Hyphantria cunea*  
107 constructs a colonial web which is heated by solar radiation, thereby generating a thermal  
108 gradient across the web (Rehnberg, 2002). Sometimes, the behavioural thermoregulation is  
109 combined with a form of intermittent endothermy (Heinrich, 1999). This process consists in the  
110 production of metabolic heat inside the structure that contributes to warming the nest. For  
111 example, the aggregation of social caterpillars of *Eriogaster lanestris* inside their nest results  
112 in a temperature increase of up to 3°C caused by metabolic heat-production (Ruf and Fiedler,  
113 2000). This process is combined with the properties of the silken nest they build to generate a  
114 favourable microclimate for larval development (Ruf and Fiedler, 2002a). To understand the  
115 effects of structure microclimate on body temperature and insect development, few researchers  
116 built biophysical models of heat exchanges. For example, the phenology of *Ips typographus*  
117 was simulated by integrating, into a development model, the bark temperature predictions  
118 derived from solar radiation as a model input (Baier et al., 2007). The thermal environment of

119 the leaf miner *Phyllonorycter blancardella* was described mechanistically by using a  
120 biophysical model which revealed high heat excess inside so small structures (Pincebourde and  
121 Casas, 2006). This biophysical approach, however, is rarely applied to insect pests, despite its  
122 potential to quantify the temperature patterns actually experienced by these pests.

123 Our objective was to characterize the microclimate in the nest of an important  
124 Mediterranean forest pest, the winter pine processionary moth (PPM), *Thaumetopoea*  
125 *pityocampa* (Denis & Schiffermüller). PPM defoliation influences the growth and vulnerability  
126 of its host plants (pine and cedar species) (Hódar et al., 2003; Carus, 2004; Parlak et al., 2019).  
127 Most importantly, urticating setae produced by late instars larvae and blown in the air or  
128 accumulated in their habitats cause sanitary problems to humans and animals due to rashes or  
129 more intense allergic reactions (Moneo et al., 2015; Battisti et al., 2017). Because periods with  
130 risk exposure and environmentally friendly solutions to manage PPM populations are life-stage  
131 dependent, the knowledge about its phenological cycle has to be improved specifically the  
132 timing of target instars depending on temperature. Furthermore, the PPM has become a model  
133 to understand the ecological impacts of climate change because its spatial distribution has  
134 readily expanded in relation to the increase of winter temperature which facilitated larval  
135 feeding and survival (Battisti et al., 2005; IPCC, 2015). Information about the thermal  
136 environment of the PPM within its nest is crucial to better understand its past and future range  
137 expansion, and to improve predictions by identifying potential invaded areas. The larvae of this  
138 species are gregarious and make their development during the cold season in a silken nest,  
139 which they leave only for feeding. We tested the hypothesis that the silken nest generates a  
140 microclimate warmer than surrounding conditions. First, we measured directly the temperature  
141 at several locations inside the nest under contrasting environmental conditions to characterize  
142 the microclimate temperature patterns experienced by larvae. We surveyed both wild nests  
143 found *in natura* and nests built by larvae previously translocated into a pine nursery. The latter  
144 approach in a nursery allowed minimizing any variance associated with individual trees, their  
145 surroundings, or the position of the nests on trees. Moreover, translocating larvae onto those  
146 experimental trees allowed manipulating and standardizing larval colony size and nest weaving  
147 effort. We expected a significant thermal heterogeneity inside the nest due to its architecture  
148 (see below). Second, we developed a biophysical model to predict the temperature inside typical  
149 PPM nests. This model should improve our understanding of the actual thermal experience of  
150 larvae as well as the mechanisms responsible for the variations of nest temperature. It is a

151 critical step towards a toolbox for realistically predicting PPM larval development rates,  
152 phenology, spread, and for forecasting sanitary risks to humans, animals and trees.

153

## 154 **2. Materials & methods**

### 155 *2.1 Study species*

156 The PPM is a univoltine species native to Southern Europe and North Africa where it  
157 occurs on evergreen trees (pines and cedars) from Mediterranean lowlands with hot summers  
158 and mild winters to mountainous areas with mild summers and cold winters. Adult emergence  
159 generally occurs during summer and larval development from summer, to next spring, both  
160 depending on weather and bioclimatic region (Battisti et al., 2015). Larvae are gregarious and  
161 go through five stages before pupation. PPM fecundity increases with latitude suggesting that  
162 larger colony size could confer an advantage for nest building at higher latitudes (Pimentel et  
163 al., 2010). Moreover, colonies are often composed of siblings issued from one egg mass. **An  
164 egg mass is composed of 70 to 300 eggs (Huchon and Demolin, 1970) with an average of 200  
165 eggs (Martin, 2005). However, a given colony** can merge with other colonies feeding on the  
166 same tree, especially at high population densities when the encounter rate increases. First instar  
167 larvae feed on needles near the egg mass where they build successive temporary nests, usually  
168 until temperatures start to decrease in fall. At this point, colonies often settle in higher branches  
169 well exposed to sunshine, where they build a durable and structured winter nest thanks to an  
170 increasing weaving effort at the third and fourth instars. Throughout their development, these  
171 larvae keep weaving silk to maintain, thicken or expand the winter nest. They stay in during the  
172 day and get out during the night to feed on needles when conditions are favourable (Huchon  
173 and Démolin, 1970; Battisti et al., 2005). At the end of larval development, they permanently  
174 leave the nest and crawl down the tree to seek a suitable pupation site in the ground, in so-called  
175 processions.

176 The PPM winter nest is a silk network with two superimposed layers. During winter, larvae  
177 continuously maintain the structural integrity of the nest. The density of the spinning increases  
178 from the external to the internal layers (Huchon and Demolin, 1970; Martin, 2005). Local  
179 climates may affect silk production: nests tend to be thicker towards northern regions and higher  
180 altitudes (Abgrall, 2001). The nest architecture creates a heterogeneous environment inside  
181 which larvae can thermoregulate behaviourally (Breuer and Devkota, 1990). Previous studies  
182 showed that temperature in the PPM nest can be higher than the environmental temperature

183 during the day (Breuer et al., 1989; Breuer and Devkota, 1990; Martin, 2005), but these studies  
184 did not provide mechanistic understanding of this temperature excess, and more detailed field  
185 measurements are needed. The hypothesis about the potential sources of this heat gain include  
186 the factors related to exposure to solar radiation (i.e., time of the day, nest localisation in tree  
187 and its orientation according to solar radiation) (Breuer and Devkota, 1990; Joos et al., 1988;  
188 Ruf and Fiedler, 2000). PPM nests are usually at the end of the main branches or at the top of  
189 the trees where they are exposed to intense solar radiation, especially at noon. Since larvae keep  
190 the same nest throughout winter, high quantities of excreta can accumulate in the lower part,  
191 but biogenic production of heat by bacteria therein was suggested to have less influence on  
192 internal nest temperature than solar radiation (Breuer and Devkota, 1990).

193

## 194 *2.2 Field sites, nest selection and nest translocation*

195 We measured the temperatures inside PPM nests in the Southern Paris Basin (France) under  
196 two conditions differing in the level of control of environmental variables that may influence  
197 the nest temperature. First, we surveyed four inhabited PPM nests selected randomly in the field  
198 in a private property at Mézières-Lez-Cléry (47.787255 N, 1.826399 E). These nests were  
199 equipped with temperature sensors (see below) but otherwise left untouched. The number of  
200 larvae inside these nests was retrospectively estimated using collar traps (Ecopiège®) to catch  
201 fifth instar larvae when they left the pine for pupation in the spring following measurements.  
202 This approach may under-estimate the number of individuals in a nest during measurements  
203 because the mortality before larvae migrated to pupate remains unknown. The number of larvae  
204 captured in collar traps ranged from 20 to 100 larvae (mean 44 larvae among the four nests).  
205 Second, we experimented on colonies collected in the field and translocated to the tree nursery  
206 of INRAE Centre Val de Loire at Orléans, France (47.832226 N, 1.911060 E). **The tree nursery**  
207 **is in an open field zone, at the edge of a forested area, in a semi-urban area (Fig. S1).** For this  
208 purpose, natural nests were collected (October 3<sup>rd</sup>, 2018) at Chaon, France (47.595665 N,  
209 2.138123 E) on black pines and translocated (October 4<sup>th</sup>, 2018) in the experimental black pine  
210 nursery. Eight days later, each nest was collected to count larvae and create eight colonies of  
211 200 caterpillars each from the overall pool of caterpillars (they were at the third and fourth  
212 larval stages). Each colony was then placed in a ventilated plastic box with fresh branches of  
213 black pine, and transferred to a climatic chamber at 12°C to promote silk weaving and the  
214 construction of a new slack nest. Ten days later (October 14<sup>th</sup>, 2019), the new nests were  
215 attached to distinct black pines at breast height (**lower branches**) in the tree nursery (each tree



216 was about 6 m high and 10 years). As expected, the colonies moved during the following days  
217 and built thicker winter nests at the top of the trees (N=8 trees). These winter nests were then  
218 equipped with temperature sensors (N=8 nests). This manipulation allowed standardizing the  
219 number of larvae inside each nest, the number of larvae contributing to the construction, and to  
220 control partially for the position of the nest inside trees (at the top of the canopy). Both  
221 experiments were conducted on black pines, *Pinus nigra*, which is among the most preferred  
222 host plant of the PPM distribution area.

223 Larvae may influence the temperature inside the nest by producing metabolic heat collectively  
224 (as observed on other tent caterpillar species; Ruf and Fiedler 2000). Therefore, in the tree  
225 nursery, we also deployed empty nests (but already ‘mature’, i.e. with dense silk layers) to be  
226 used as controls for the effect of larval presence. To remove larvae from natural nests without  
227 altering its structure, we put nests in plastic boxes and placed them in a climatic chamber at  
228 30°C for one week. Larvae left the nests naturally and the resulting empty nests were then  
229 translocated in the tree nursery, and equipped with temperature sensors (N=3 nests) from  
230 February 1<sup>st</sup> to March 20<sup>th</sup>, 2019.

231

### 232 *2.3 Temperature measurements*

233 We determined the temperature inside the PPM nests and calculated the difference between this  
234 temperature and air temperature, i.e. the nest temperature excess ( $T_{excess} = \text{Nest temperature}$   
235 ( $T_n$ ) – Air temperature ( $T_a$ )), in each nest at the two sites. In November 2018, five thermocouples  
236 (Copper-Constantan, type T, 0.2mm in diameter, TCESA, Dardilly, France) were installed in  
237 each nest. Three thermocouples were positioned at different locations inside the nest (top,  
238 middle and lower parts, respectively) and two others were fixed in the external layer of silk, at  
239 the surface, on northern and southern sides of the nest. The fifth thermocouple was deployed  
240 on the same branch as the nest to measure air temperature in the shade near the nest. The  
241 thermocouples (5 m length) were connected to two weather stations (CR1000, Campbell  
242 Scientific Ltd, Leicestershire, UK) equipped with a multiplexer (AM25T, Campbell Scientific  
243 Ltd) allowing to connect up to 25 thermocouples each. The temperature sensors were set to  
244 record temperatures every 5 minutes over winter, between November 2018 and May 2019. To  
245 record the timing of larval processions, a collar trap (Ecopiège®) was installed on each tree  
246 trunk to intercept larvae on their way down for pupation (see Colacci et al., 2018 for more  
247 details on this method). These collar traps were checked every two weeks between February

248 2019 and May 2019. In addition, global radiation ( $\text{W.m}^{-2}$ ) and wind velocity ( $\text{m.s}^{-1}$ ) were  
249 recorded throughout the experiments from a weather station located less than 500 m away from  
250 the INRAE tree nursery.

251

#### 252 *2.4 Metabolic heat estimation*

253 The production of metabolic heat by PPM larvae was estimated indirectly by measuring  
254 temperature in small containers containing a given number of caterpillars depending on ambient  
255 temperature and larval density. This method allowed estimating the influence of larval presence  
256 on air temperature inside a small volume, especially under cold conditions. Larvae were  
257 collected in the Orléans surrounding and randomly placed in 150 mL plastic containers to test  
258 two ambient temperatures (5 and 25°C) and six larval densities (0, 1, 5, 25, 50 and 100 larvae)  
259 under controlled conditions. All containers were closed. A datalogger (TidbiT V2, HOBO)  
260 programmed to sample temperature every minute for one hour was placed at the bottom of each  
261 container, in contact with the larvae.

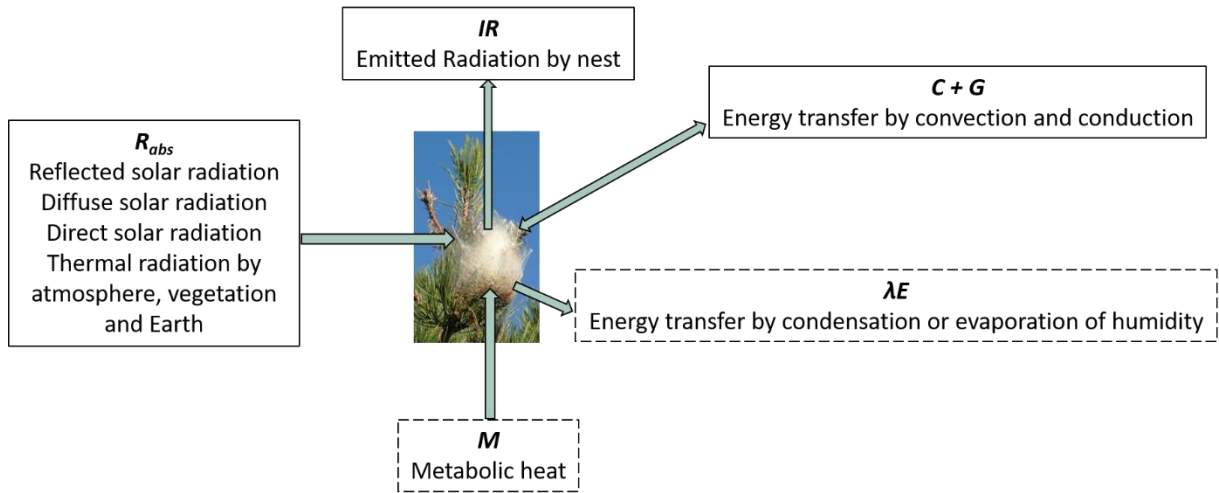
262

#### 263 *2.5 Biophysical modelling*

264 We developed a simple biophysical model to predict the PPM nest temperature from  
265 environmental variables and nest properties (Table 1). Assuming that nest temperature is  
266 determined by heat transfer between the nest and its surrounding (all the equations were derived  
267 from Gates and Schmerl, 1980), the energetic balance can be described by:

$$268 \quad R_{abs} + (C + G) + IR + \lambda E + M = 0 \quad (1)$$

269 Here,  $R_{abs}$  is the amount of radiation absorbed by the surface of the nest ( $\text{W.m}^{-2}$ );  $C$  and  $G$  are  
270 heat transfers by convection and conduction, respectively ( $\text{W.m}^{-2}$ );  $IR$  is the radiation emitted  
271 by the nest surface ( $\text{W.m}^{-2}$ );  $\lambda E$  is the transfer by evaporation or condensation of humidity ( $\text{W.m}^{-2}$ );  
272  $M$  is the metabolic heat ( $\text{W.m}^{-2}$ ). Those fluxes can be positive or negative depending on the  
273 direction of the heat transfer (gained or lost by the nest, respectively) (Fig. 1). In the model,  
274 evaporation was neglected because insect water reserves are too small to compensate  
275 overheating by evaporation (May, 1979), and we considered the nest as a dry structure. The  
276 production of metabolic heat was low in our experiment (see results), and therefore this  
277 production was neglected in our model ( $M = 0$ ). Below, we provide the details for each term of  
278 the equation (1).



279

280 **Figure 1.** Schematic representation of heat fluxes involved in the energetic budget of a PPM  
 281 nest. Arrows: direction of heat fluxes. Dashed boxes: fluxes that were neglected in our model.

282

283 The nest emits long wave infrared radiation according to the Stefan-Boltzmann law:

$$284 \quad IR = \varepsilon_n \sigma T_n^4 \quad (2)$$

285 where  $\varepsilon_n$  is the emissivity of the nest's surface,  $\sigma$  the Stefan-Boltzmann radiation constant ( $\sigma =$   
 286  $5.673 \cdot 10^{-8} \text{ W}\cdot\text{m}^{-2}\cdot\text{K}^4$ ), and  $T_n$  the absolute temperature of the nest. The nest emissivity was  
 287 estimated using an infrared camera (FLIR Systems B335; Wilsonville, OR) and a thermocouple  
 288 (copper-constantan type T) at the same time. A piece of silk was placed on a metallic plate  
 289 heated by a bowl of hot water. The thermocouple was applied against the silk layer. The  
 290 emissivity value was adjusted in the settings of the camera until the temperature recorded by  
 291 the camera reached the value recorded by the thermocouple. The silk emissivity (0.5) was found  
 292 when the two temperatures were equal.

293 The PPM nest absorbs direct, reflected and scattered solar radiation plus long wave infrared  
 294 radiation from the atmosphere, the vegetation and the ground. The nest absorbs in the visible  
 295 and near infrared as follows:

$$296 \quad R_{abs} = a^{VIS} 0.48 R_{ad} + a^{NIR} 0.52 R_{ad} + \varepsilon_a \sigma T_a^4 \quad (3)$$

297

298 where  $R_{ad}$  is the global radiation ( $\text{W}\cdot\text{m}^{-2}$ ); corresponds to the emissivity of the atmosphere, and  
 299  $T_a$  is the absolute air temperature.  $a^{VIS}$  and  $a^{NIR}$  represent the nest absorbance in the visible  
 300 (0.60) and near infrared (0.25), respectively, that we estimated from absorbance measurements

301 made on the natural silk fibers of insects like *Bombyx mori* (Balčytis et al., 2017). We hereby  
302 assume that all the elements in the environment of the nest have the same temperature than  
303 ambient air.

304 The heat transfer from the nest to atmosphere by conduction and convection is:

$$305 \quad C + G = C_p g_h (T_a - T_n) \quad (4)$$

306  $C_p$  is the specific heat of the air ( $C_p = 29.3 \text{ J.mol}^{-1}.\text{°C}^{-1}$ ),  $g_h$  is the nest boundary layer  
307 conductance, calculated as follows:

$$308 \quad g_h = 0.135 \sqrt{\frac{\mu}{d}} \quad (5)$$

309 which depends on wind velocity  $\mu$  and on nest characteristic dimension  $d$ . The factor 0.135 is  
310 obtained after integrating the values of air viscosity, air density and air diffusivity (Campbell  
311 and Norman, 1998). The PPM nest can be assimilated to an ellipsoid, giving for the  
312 characteristic dimension:

$$313 \quad d = 0.7 L \quad (6)$$

314 where  $L$  is the higher axis of the ellipsoid. In this model, the thermal inertia of the nest was  
315 considered negligible, allowing us to provide a simple version that considers the nest as a  
316 surface element (but see discussion for potential limitations).

317

## 318 *2.6 Model simulations and validation*

319 This model was coded in the R language (R Core Team 2018) and is provided in the  
320 supplemental material S1. Temperature inside the nest was simulated based on air temperature  
321 and global radiation recorded from November 2018 to May 2019. Then, the deviation between  
322 simulated and observed nest temperatures was calculated based on the Mean Absolute Error  
323 (MAE), as a measure of accuracy of the biophysical model.

324 The influence of air temperature and global radiation was quantified by running a simple  
325 sensitivity analysis of the model. To evaluate the effect of air temperature, the nest temperature  
326 predicted by the model was calculated for constant air temperatures 5, 10, 15, 20, 25 and 30°C  
327 with a fixed global radiation at either high level (750 W.m<sup>-2</sup>) or low level (158.3 W/m<sup>2</sup>). To  
328 assess global radiation effect, the nest temperature was predicted using constant global radiation

329 at 125, 250, 375, 500, 625 and 750 W.m<sup>-2</sup> and setting air temperature to either 0 or 25°C. These  
330 radiation levels reflect common values in our geographical area (Pincebourde and Casas 2006).

331 Finally, we assessed the effect of climate warming on nest temperature to test if the amplitude  
332 of nest warming corresponds to the amplitude of climate warming. We ran the biophysical  
333 model by adding 2 and then 5°C to the air temperature pattern recorded with the weather station  
334 at our study site (Orléans) during the experiment. The other parameters and variables were not  
335 changed.

336

### 337 *2.7 Statistical analyses*

338 A non-parametric test of Mann-Kendall was used to analyse the difference between air and nest  
339 temperatures, and the positive correlation between global radiation and nest temperature. To  
340 test the effects of caterpillars' presence inside the nest (i.e., empty versus occupied nest), the  
341 thermocouple position (i.e., within nest thermal heterogeneity), and the interaction between  
342 those two factors, we used a repeated measure ANOVA with the nest temperature excess as  
343 response variable. A non-parametric test of Kruskal-Wallis was used to analyse the effect of  
344 thermocouple position on the recorded nest temperature. We quantified the accuracy of the  
345 biophysical model by calculating the Mean Absolute Error (MAE) with the *mae* function of the  
346 R package *Metrics*. R 3.5.1 was used for statistical analyses (R Core Team 2018).

347

348

349

350

351

352

353

354

355

356

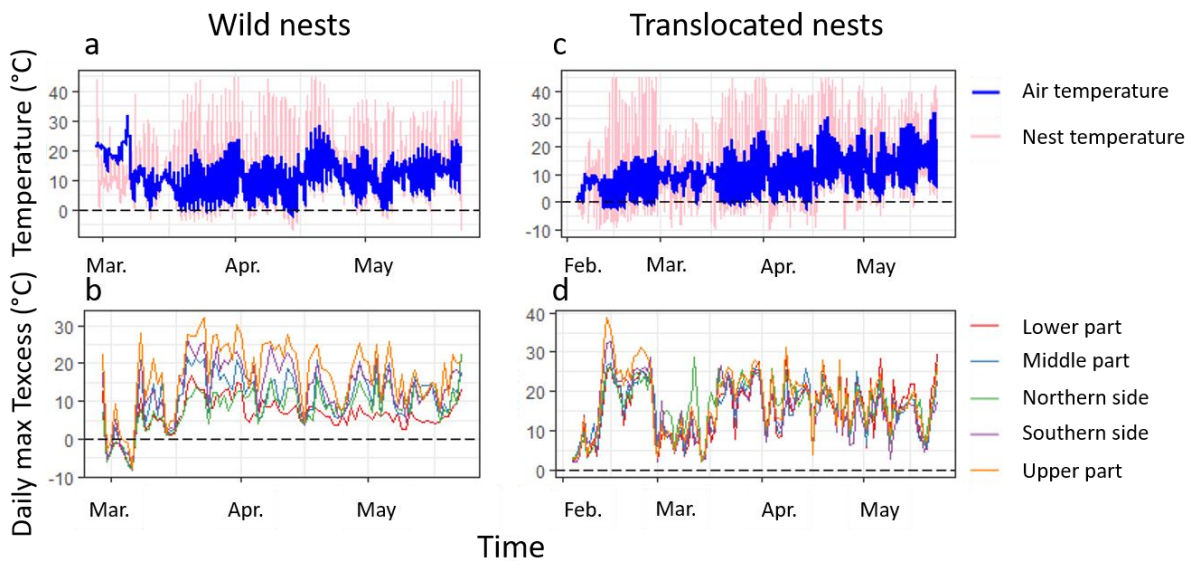
357 **Table 1:** List of the parameters involved in the biophysical model.

<i>Parameters</i>	<i>Symbol in equations</i>	<i>Values (units)</i>	<i>Sources</i>
Nest emissivity	$\varepsilon_n$	0.5	Field measurement
Atmosphere emissivity	$\varepsilon_a$	0.77	Campbell and Norman, 1998
Nest characteristic dimension	$d$	0.06 m	Field measurement
VIS nest absorbance	$a^{VIS}$	0.60	Balčytis et al., 2017
NIR nest absorbance	$a^{NIR}$	0.25	Balčytis et al., 2017
Global radiation	$R_{ad}$	20 to 577.78 W.m <sup>-2</sup>	Field measurement
Air temperature	$T_a$	-2.45 to 31.74°C	Field measurement
Wind velocity	$\mu$	0 to 6 m.s <sup>-1</sup>	Field measurement
Nest temperature	$T_n$	-6.5 to 44.5°C	Field measurement
Stefan-Boltzmann radiation constant	$\sigma$	5.673 10 <sup>-8</sup> W.m <sup>-2</sup> .K <sup>4</sup>	Campbell and Norman, 1998
Specific heat of the air	$C_p$	29.3 J.mol <sup>-1</sup> .°C <sup>-1</sup>	Campbell and Norman, 1998

358 **3. Results**

359 *3.1 Observed deviations between air and nest temperatures*

360 In all nests (whether they are occupied by larvae or empty), temperature varied greatly  
361 according to the time of the day (Fig. 2a and 2c). Globally, regardless of the thermocouple  
362 position, nest temperature exceeded air temperature at noon but was very similar and sometimes  
363 lower than air temperature during night (Fig. 2b and 2d). For wild nests, maximal air  
364 temperature and maximal nest temperature (considering all nests and thermocouple positions)  
365 were 31.74°C and 44.5°C, respectively (Fig. 2a). For translocated nests, maximal temperatures  
366 were marginally higher, at 32.25°C for air and 44.98°C for nests (Fig. 2c). The nest temperature  
367 was positively correlated to the air temperature (Mann-Kendall p-value < 0.001, Rho = 0.67 for  
368 wild nests and p-value < 0.001, Rho = 0.76 for translocated nest). As expected, the nest  
369 temperature was positively correlated to global radiation (Mann-Kendall p-value < 0.001, Rho  
370 = 0.31 for wild nests and p-value < 0.001, Rho = 0.19 for translocated nests).



371

372 **Figure 2.** Air and nest temperatures when considering all thermocouple positions (°C) recorded  
373 in wild (a) and translocated nests (c). Daily maximal Texcess (°C) for each thermocouple  
374 position in wild (b) and translocated (d) nests.

375

376 Temperature was not homogeneous inside nests, neither for wild nor translocated nests (Fig. 2b  
377 and 2d). The temperature gradient inside nests, as inferred according to the position of  
378 thermocouples, was significant (RM ANOVA p-value < 0.001). For all wild nests, temperature

379 was higher in the upper part of the nest (mean daily maximal  $T_{\text{excess}} = 17.12^{\circ}\text{C}$ ) than in the  
380 middle ( $11.03^{\circ}\text{C}$ ) and in the lower part ( $6.39^{\circ}\text{C}$ ) (Kruskal-Wallis p-value  $< 0.01$ ) (Fig. 2b). A  
381 similar pattern was observed in translocated nests ( $17.53$ ,  $15.48$  and  $15.30^{\circ}\text{C}$  for upper, middle  
382 and lower parts, respectively; Fig. 2d), although the spatial gradient was less marked. Empty  
383 nests also displayed a significant internal temperature heterogeneity (Fig. S2). On average and  
384 globally (all thermocouples considered), the maximal  $T_{\text{excess}}$  was higher in translocated nests  
385 than in wild and empty nests ( $16.47$ ,  $11.23$ , and  $14.75^{\circ}\text{C}$ , respectively; **overall mean of  $16^{\circ}\text{C}$** ).  
386 The internal temperature (averaged from all thermocouples) significantly differed between nest  
387 types (translocated, wild, empty; Kruskal Wallis, p-value  $< 0.001$ ). Air temperature recorded at  
388 the two sites (i.e. the site with translocated nests and the one with wild nests) was similar (Mann-  
389 Kendall p-value  $< 0.001$ ,  $Rho = 0.66$ , average of  $9.28^{\circ}\text{C}$  and  $11.26^{\circ}\text{C}$  respectively) and therefore  
390 does not explain the temperature difference among nest types.

391

### 392 *3.2 Estimating heat production by larvae*

393 Heat production by larvae was found to be relatively negligible at all colony densities and  
394 ambient temperatures tested. Overall, the mean thermal difference between containers with  
395 larvae and empty containers (i.e., temperature in occupied containers minus temperature in  
396 empty containers) was very low ( $-0.02^{\circ}\text{C}$ ), ranging from  $-1.57^{\circ}\text{C}$  (container with density 50  
397 larvae in the warm treatment was  $1.57^{\circ}\text{C}$  colder than the control) to  $0.99^{\circ}\text{C}$  (density 100 larvae  
398 in the cold treatment, almost  $1^{\circ}\text{C}$  warmer than the control). These deviations were small and  
399 the sign of the difference was relatively erratic among the density treatments, potentially due to  
400 the lack of control of the contact point between the logger and the caterpillar(s) or of the  
401 humidity within the containers. Therefore, larval presence barely influenced the temperature  
402 within small volumes. These deviations (between  $1$  and  $2^{\circ}\text{C}$ ) were deemed negligible compared  
403 to the amplitude of the nest temperature excess (see Fig. 2).

404

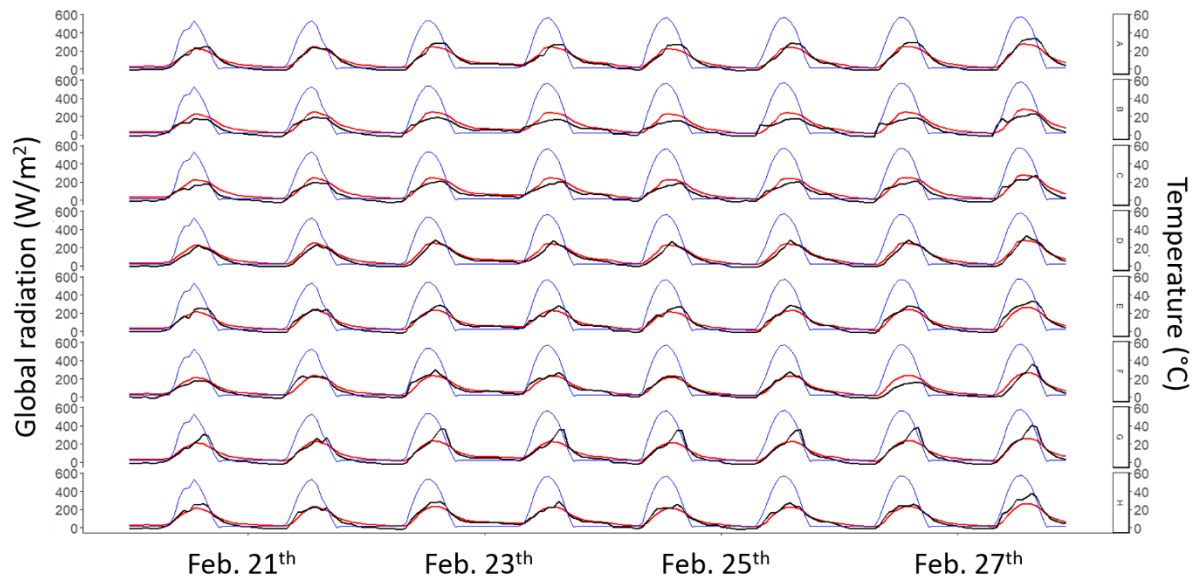
### 405 *3.3 Model validation*

406 The nest temperature predicted by the model was positively correlated with the nest temperature  
407 recorded in the field (Pearson's  $r > 0.9$ , p.value  $< 0.001$ ) (Fig. 3 and 4). Our model does not  
408 predict temperature inside distinct nest parts with the same accuracy. The MAE were  $4.31$ ,  $4.86$ ,  
409  $5.25$ ,  $5.20$  and  $5.00^{\circ}\text{C}$  for the lower part, middle part, northern surface, upper part, and southern



410 surface, respectively. Overall, the error of the model can be both positive (over-estimate) and  
411 negative (under-estimate), although there is a tendency to overestimate the nest temperature  
412 more often (Fig. 4).

413

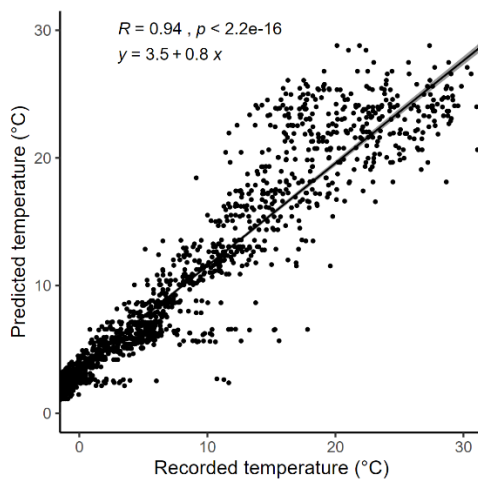


414

415

416 **Figure 3.** Temperature predicted inside nests by the biophysical model (red) and temperature  
417 recorded at the lower part of these nests (black) for a one-week period with clear sky (cloudless).  
418 Blue: Global Radiation ( $\text{W}/\text{m}^2$ ). Letters: Nest IDs.

419



420

421 **Figure 4.** Performance of the biophysical model when combining all nest types. Pearson's  
422 correlation between predicted nest temperature and recorded temperature at the lower part of  
423 the nest, for the week from February 20<sup>th</sup> to February 28<sup>th</sup>.

424

425

### 3.4 Role of air temperature and global radiation: sensitivity analysis

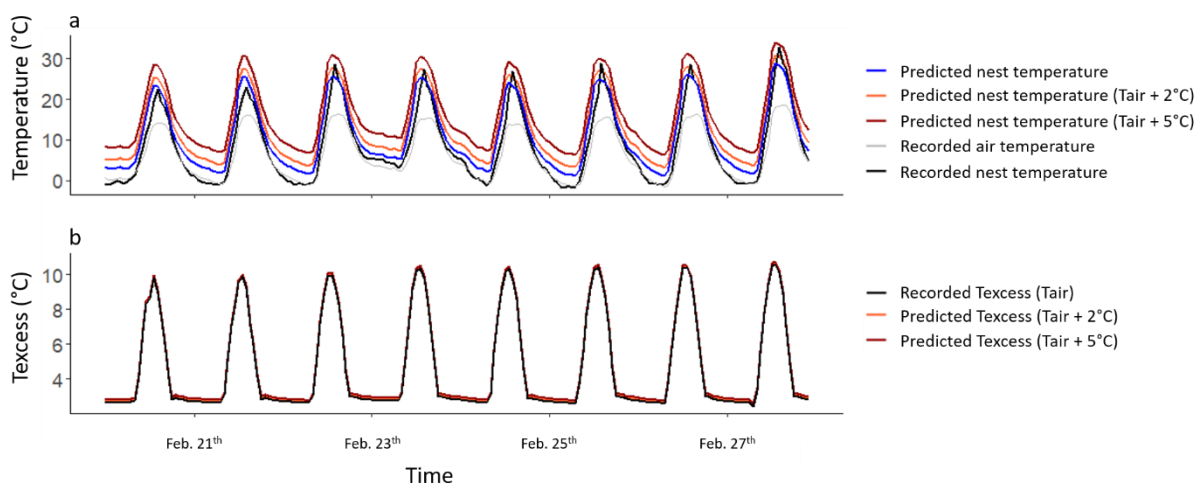
426 Air temperature was the most influential variable on nest temperature predicted by the model.  
427 When air temperature increased from 5 to 30°C, the nest temperature estimated by the model  
428 increased linearly from 16.2 to 42°C at high global radiation of 750 W.m<sup>-2</sup>, and from 9.38 to  
429 35.31°C for a low global radiation level of 158.3 W.m<sup>-2</sup> (Fig. S3, slope = 1.03 for both radiation  
430 levels). By contrast, when air temperature was fixed at 25°C and the global radiation increased  
431 from 125 to 750 W.m<sup>-2</sup>, the predicted nest temperature increased linearly but more slowly from  
432 29.73 to 36.82°C (from 3.88 to 11.07°C when air temperature was fixed at 0°C) (Fig. S4, slope  
433 = 0.01 for both air temperatures).

434

### 3.5 Simulation of warming

436 The model was used to predict the nest temperature response to an increase in air temperature.  
437 With an increase of air temperature by 2°C (T<sub>air</sub> + 2°C) and 5°C (T<sub>air</sub> + 5°C) in the natural air  
438 temperature trace measured at our study site (T<sub>air</sub>) from February 20<sup>th</sup> to February 28<sup>th</sup>, the  
439 mean temperature of the lower part predicted by the model was respectively 12.31°C and  
440 15.42°C (Fig. 5a) for the period. The nest temperature excess during an increase of air  
441 temperature by 2°C and 5°C (4.47 and 4.57°C, respectively) was similar to the actual  
442 temperature excess recording for the same period (4.40°C) (Fig. 5b).

443



444

445 **Figure 5.** Model simulations for temperature in the lower part of the nest during one week of  
446 the experiment (a). Predicted nest temperature excess based on actual air temperature  
447 recordings ( $T_{air}$ ) for the same period and for air temperature + 2°C and + 5°C (b).

448

#### 449 4. Discussion

450 Ectotherms live in microhabitats that often provide particular thermal environments  
451 (Willmer, 1982). The thermal heterogeneity at very fine spatial scale can be exploited by  
452 arthropods to increase their survival and fitness (e.g., Pike et al., 2012; Caillon et al., 2014). We  
453 quantified the microclimatic temperature of the winter nest of the PPM, an increasing forest  
454 and human health concern in the context of global changes. We show that during winter,  
455 temperature within the nest can be much higher than ambient air temperature, **by 16°C on**  
456 **average**, when exposed to intense solar radiation on a cloudless day. Therefore, the winter nest  
457 may provide benefits in terms of development by exposing larvae to higher temperatures during  
458 the cold season that generally slows down development rates of insects (Sinclair et al., 2016),  
459 and by decreasing the frequency of experienced temperatures below developmental or feeding  
460 thresholds (Battisti et al., 2005; Robinet et al., 2007). Nevertheless, our results indicate that the  
461 hot nest of the PPM cannot help the caterpillars to overcome the cold challenge imposed by  
462 winter during night time, which is the daily period with lowest temperatures, for two reasons:  
463 metabolic heat production may be insignificant and the nest warms up only when exposed to  
464 radiation (combined with a low thermal inertia). In areas where the climate is not close to the  
465 limits of the species, the net advantage or disadvantage of living in a warm nest during winter  
466 remains to be determined as it is unknown if the resulting phenological changes would be  
467 beneficial, maladaptive, or buffered in this univoltine species.

468 The temperature inside the silken nest differs from air temperature, thereby confirming  
469 a previous study in Mont Ventoux (Southeast of France) during which the temperature excess  
470 reached 21°C in four nests taken in the wild (Martin, 2005). Breuer *et al.* (1989) measured  
471 temperature inside 28 nests in Greece according to their volume and thickness. The highest  
472 temperature excess was obtained at noon and was >15°C (Breuer et al., 1989). This  
473 phenomenon is also observed in other lepidopteran species like in the small eggar, *Eriogaster*  
474 *lanestris* (Ruf and Fiedler, 2000). Larvae inside the nest experience conditions warmer than  
475 surrounding temperature, mostly due to the production of collective metabolic heat in this  
476 particular case (Ruf and Fiedler, 2000). Indeed, the nests of the PPM and other tent caterpillars

477 like *E. lanestris* differ in their main function. The nest of *E. lanestris* is made of silk that reflects  
478 incoming radiation so that the nest does not absorb much radiative energy, and the metabolic  
479 heat produced by larvae (Ruf and Fiedler, 2002a) mainly adjusts the temperature excess inside  
480 the nest. By contrast, we showed that temperature in the PPM nest depends mostly on global  
481 radiation received. We found little support for the production of metabolic heat by larvae. This  
482 difference can be explained by the activity rhythms and the season: during summer, *E. lanestris*  
483 are active and exit the nest during the day, and they rely on metabolic heat during the night to  
484 keep it warm (Ruf and Fiedler, 2002a). By contrast, the PPM remains in the winter nest during  
485 the day, **even when temperatures inside the nest reach  $>40^{\circ}\text{C}$  (Breuer et al., 1989)**, and leaves  
486 it to feed during nighttime. **This indicate that nest temperature may induce thermal stress during**  
487 **the winter due to elevated nest temperatures (e.g. we measured nest temperatures up to  $40^{\circ}\text{C}$ ),**  
488 **but the thermal biology of this species remained poorly documented.** We report nest  
489 temperature excess of  $>10^{\circ}\text{C}$  relative to ambient air during day-time. Interestingly, this  
490 temperature excess is similar to that of a much smaller insect structure, such as leaf mines which  
491 also partly rely on incoming solar radiation that warms up the structure (Pincebourde and Casas,  
492 2006). This temperature excess has profound influence on the development rate and survival of  
493 these leaf miners (Pincebourde et al., 2007). This demonstrates that the microclimate created  
494 by the nest during winter has to be considered to understand PPM larval development. PPM  
495 feeding activity was shown to occur if a daytime nest temperature exceeds  $9^{\circ}\text{C}$  and air  
496 temperature exceeds  $0^{\circ}\text{C}$  during the following night (Battisti et al., 2005). We hypothesize that  
497 the exposure to warmth during daytime in the winter nest optimizes assimilation rates,  
498 allocation of nutrients to somatic growth, and therefore overall growth rate.

499 Nest temperature is higher than ambient air, especially around noon when the global  
500 radiation is maximal. In dense forest stands, nest number is known to be much higher at south-  
501 orientated stand edges (Samalens and Rossi, 2011; Jactel et al., 2015). Moreover, a study on  
502 the position of the PPM winter nest in a tree demonstrated that PPM larvae prefer building the  
503 nest at the top of trees where exposure to solar radiation is high (Breuer et al., 1989). As in this  
504 study, we found a positive correlation between the PPM nest temperature and the global  
505 radiation. In the eastern tent caterpillar (*Malacosoma americanum*), one of the mechanisms  
506 involved in the heat gain is also related to absorption of global radiation (solar radiation and  
507 radiation emitted by the nest) (Fitzgerald et al., 2012). Again, this absorption of incident global  
508 radiation is probably even more important for the PPM, whose larval development is slowed

509 down by winter conditions. The silk of the PPM nest seems to absorb solar radiation. However,  
510 the properties of the silk nest to absorb visible and near infrared radiation remain to be detailed.

511 On average, the translocated nests reached higher temperatures than the wild nests. The  
512 greater mean of daily maximal temperature excess recorded in translocated nests may be due to  
513 their position in the trees. During the experiment, translocated nests with caterpillars were all  
514 at the top of the trees, whereas empty and wild nests were slightly lower in the canopy.  
515 Furthermore, empty nests were slightly warmer than wild nests, which refuted our hypothesis  
516 that larval metabolic heat could be involved in the heat excess of the nest. It is possible that  
517 empty nests were less exposed to wind than wild nests because they were in the middle of a  
518 pine nursery whereas wild nest were located at the periphery of the forest stand. The wind speed  
519 is known to influence the loss of heat by convection (Breuer et al., 1989; Joos et al., 1988;  
520 Ronnås et al., 2010). The number of caterpillars within the nest can affect nest temperature  
521 (Joos et al., 1988; Ruf and Fiedler, 2002a). Indeed, we found that the temperature **excess** in  
522 wild nests (20-100 individuals) was lower than in the translocated nests (200 individuals). The  
523 net increase in nest temperature during the day under solar radiation may be an alternative to  
524 heat up the nest without losing energy to produce metabolic heat.

525 Our model underestimated nest temperature for some of the nests we followed,  
526 indicating a potential effect of metabolic heat. However, we did not detect metabolic heat  
527 production from our temperature measurement in the nursery when comparing empty and  
528 occupied nests. Collective metabolic heat may exist in the PPM but its impact on the nest  
529 temperature is certainly buffered by the other components of the heat budget. Supportingly, a  
530 previous study indirectly inferred that the presence of larvae in the nest influences internal  
531 temperature by less than 1.5°C (Breuer and Devkota, 1990), a different order of magnitude  
532 compared to the influence we found for other factors. Our model overestimated nest  
533 temperature for other nests we followed. This tendency could suggest an effect of evaporation,  
534 since our model simulated a dry nest. However, evaporation was shown to have a minimal  
535 influence compared to global radiation and convection (Breuer et al., 1989). Other factors like  
536 the thickness of the silk can influence the temperature pattern (Breuer et al., 1989; Fitzgerald et  
537 al., 2012). Thickness changes over winter as the larvae continuously develop the nest – a  
538 dynamics that is not included into the biophysical model. In addition, the accumulation of faeces  
539 at the bottom of the nest may play a role in the nest temperature increase by capturing some of  
540 the incoming radiation and/or by favouring bacterial development and the production of heat  
541 (Battisti et al., 2005). Finally, winter precipitations may also interact on the nest heat budget

542 by adding water to the structure, thereby permitting evapotranspiration following rain events,  
543 but this effect was never tested. Thus, to improve the predictions of nest temperature by the  
544 biophysical model, the effect of those factors should be considered. Our model should be seen  
545 as a simulator of an average and static nest, but nest properties are quite variable in the field  
546 and they may be adjusted in the field according to season and weather conditions.

547         A significant thermal gradient was found in the PPM nest, generally from the bottom to  
548 the top. Deviations of  $>15^{\circ}\text{C}$  were often recorded among the different locations inside the same  
549 nest. This gradient can be explained by the major impact of solar radiation at the top of the nest  
550 and by the position of caterpillars (generally in the upper part of the nest) (Joos et al., 1988; Ruf  
551 and Fiedler, 2000). We found that translocated nests were less thermally heterogeneous than  
552 wild nests, probably because they were more exposed to direct solar radiation, thereby  
553 homogenizing somehow the temperature at the scale of the nest and they contained more larvae  
554 to maintain nest structure thereby limiting heat loss. Therefore, the caterpillars can potentially  
555 move across the nest to thermoregulate behaviourally, but we currently lack evidence of such  
556 behaviour at the scale of the nest. Behavioural thermoregulation across very fine spatial scales  
557 was demonstrated for spider mites moving across single leaf surfaces that display thermal range  
558 of up to  $10^{\circ}\text{C}$  (Caillon et al., 2014). A similar process was found for flat rock spiders in  
559 challenging environments in Australia, with the female and its offspring using a gradient of  
560  $15^{\circ}\text{C}$  across only few centimeters (Pike et al., 2012). In other tent caterpillars, the larvae were  
561 observed to leave their nest and use the temperature heterogeneity of the silk surface to regulate  
562 their body temperature (Ruf and Fiedler, 2002). Some observations were made indicating that  
563 PPM larvae exit the nest during hot days, but more detailed observations of caterpillar  
564 behaviour are needed to test this hypothesis. We propose that the PPM larvae could benefit  
565 from this nest thermal heterogeneity by moving up (warmer spots) during cold periods and  
566 down (cooler spots) during heat wave events.

567

## 568         **5. Conclusion**

569         Environmental warming is expected to influence the PPM nest microclimate. Our  
570 simple approach using the biophysical model allows inferring that the amplitude of warming  
571 inside the nest will likely follow the amplitude of warming in the atmosphere, assuming that  
572 global radiation and the nest properties remain unchanged. This result contrasts with other  
573 studies reporting that the microhabitat of some species (e.g., leaf miners, mussels on rocky

574 shores) allow them to buffer partially the amplitude of warming in the air – i.e., the temperature  
575 excess in the structure diminishes slightly with air temperature increasing (Pincebourde and  
576 Casas 2006; Gilman et al. 2006). This buffering is often linked to the evapotranspiration  
577 process, which was considered to be negligible in the PPM biophysical model, although we  
578 cannot exclude that evaporation can occur after precipitation events and also due to the presence  
579 of needles in the nest. Environmental warming will therefore be transferred into the PPM winter  
580 nest. The thermal tolerance thresholds of PPM caterpillars are not known, but given that they  
581 inhabit the permanent nest during the cold season, we propose that the microclimate warming  
582 will benefit to larval development rate and alleviate to some extent the cold stress constraint,  
583 especially near elevational and north range fronts. Many insect pest species build structures or  
584 develop inside particular microhabitats such as plant tissues (fruits, wood, and leaf tissues). The  
585 PPM nest creates a novel thermal niche, by producing a warm microclimate that could promote  
586 larval development during unusually cold years and facilitate survival in otherwise too  
587 challenging areas near the northern or altitude fronts of this range-expanding species.

588 Our results can help to generalize on the functions of silk nests in gregarious  
589 Lepidopteran species. Most species of the *Thaumetopoeinae* subfamily build more or less  
590 structured nests (Battisti et al. 2017) despite varied phenologies and climates, and other species  
591 within the *Thaumetopoea* genus weave silken nests during the cold season, such as  
592 *Thaumetopoea wilkinsoni* (Roques, 2015). The potential functions of the nest range include  
593 protection against natural enemies and/or dislodgment and promoting the maintenance of  
594 gregarious behaviours which may be important in the ecology of the species (de Boer and  
595 Harvey, 2020), such as feeding activity or dispersal. In the PPM, several observations suggest  
596 that the microclimatic function of the winter nest can be plastic. First, silk density and PPM  
597 nest thickness tend to decrease from harsh bioclimatic regions (North, more continental) to less  
598 stringent bioclimatic regions (South, oceanic), despite higher enemy pressures in historic  
599 compared to neocolonized regions (Démolin, 1965; Martin, 2005; Georgiev et al. 2020).  
600 Second, in a unique Portuguese population of *T. pitocampa* known for its atypical summer  
601 development, larvae were found to invest less energy in silk production than larvae from  
602 surrounding typical winter populations, resulting in loose and unstitched nests (Démolin, 1965;  
603 Santos et al., 2007). Loose silk nests are also observed in other closely related species  
604 completing their larval development between spring and summer, such as *Thaumetopoea*  
605 *ispartaensis*. Other species with larval development in spring do not build any silken nest, like  
606 *Thaumetopoea pinivora*. To avoid overheating, these spring larvae shuttle around the tree trunk

607 between shade and sunny places (Roques, 2015). Although a correlation between climate and  
608 tendency to build a silk nest remains to be explored, we propose that the hot microclimate is a  
609 fundamental nest function in species with winter larval development to enhance development  
610 and survival. By contrast, other functions such as protection against parasitoids and some  
611 predators may be more likely for species with spring and summer larval development.  
612 Additional thermal ecology studies are needed to test this hypothesis.

613 As PPM nests can shelter other arthropod species, this novel thermal niche may also  
614 play a role for some of them (concept of ecosystem engineers), especially for some non-web-  
615 building spiders (Branco et al., 2008). A similar thermal mechanism may hold for all insects  
616 developing within fruits like *Drosophila suzukii* or the codling moth. The temperature within  
617 fruits can be higher than ambient air (Saudreau et al., 2009) and some pests on apple exploit  
618 this thermal heterogeneity. Nevertheless, insect pest management programs only rarely  
619 consider the thermal environment actually experienced by those insects in the field. Identifying  
620 the microclimatic temperature that insect pests actually experience would help resolving the  
621 influence of atmospheric temperature changes on their development rate, their phenology, and  
622 ultimately on their demography and distribution with climate change.

623

624



625 **Acknowledgements**

626 We greatly acknowledge Walter Lapertot for the authorization to use his pine plot and Patrick  
627 Pineau for his technical assistance. We thank Météo-France and the AgroClim unit from  
628 INRAE for providing hourly global radiation and wind speed data. The study was made  
629 possible thanks to the financial support from the Centre Val de Loire Region (L.P.'s PhD  
630 grant), and the French National Research Agency (ANR) in the frame of the project called  
631 PHENEC.

632

633 **Funding**

634 Centre Val de Loire Region for thesis funding and ANR PHENEC [grant number19-CE32-  
635 0007-04].

636

637 **Conflicts of interest**

638 The authors declare no conflicts of interest.

639

640 **Availability of data and material**

641 The datasets collected and used to build the biophysical model of the nest are available from  
642 the corresponding author on request.

643

644 **Code availability**

645 In supplemental materials.

646

647 **Authors' contributions**

648 Conceptualization and experimental design: LP, ML, SP, CR, JR, CS. Sampling, experiments  
649 and monitoring: LP, SP. Data and statistical analyses: LP, SP. Original draft writing and  
650 preparation: LP, SP. Review and final editing: LP, ML, SP, CR, JR, CS. All authors have read  
651 and agreed to the final version of the manuscript.

652 **References**

- 653 Abgrall, J.F., 2001. Le réseau surveillance processionnaire du pin en France 1969-1989 :  
654 Conception, historique, résultats. IRSTEA, pp.400.
- 655 Baier, P., Pennerstorfer, J., Schopf, A., 2007. PHENIPS—A comprehensive phenology model  
656 of *Ips typographus* (L.) (Col., Scolytinae) as a tool for hazard rating of bark beetle  
657 infestation. *Forest Ecology and Management* 249, 171–186.  
658 <https://doi.org/10.1016/j.foreco.2007.05.020>
- 659 Balčytis, A., Ryu, M., Wang, Xuewen, Novelli, F., Seniutinas, G., Du, S., Wang, X., Li, J.,  
660 Davis, J., Appadoo, D., Morikawa, J., Juodkazis, S., 2017. Silk: Optical Properties  
661 over 12.6 Octaves THz-IR-Visible-UV Range. *Materials* 10, 356.  
662 <https://doi.org/10.3390/ma10040356>
- 663 Battisti, A., Avci, M., Avtzis, D.N., Jamaa, M.L.B., Berardi, L., Berretima, W., Branco, M.,  
664 Chakali, G., El Alaoui El Fels, M.A., Frérot, B., Hódar, J.A., Ionescu-Mălăncuș, I.,  
665 İpekdağ, K., Larsson, S., Manole, T., Mendel, Z., Meurisse, N., Mirchev, P., Nemer,  
666 N., Paiva, M.-R., Pino, J., Protasov, A., Rahim, N., Rousselet, J., Santos, H., Sauvard,  
667 D., Schopf, A., Simonato, M., Yart, A., Zamoum, M., 2015. Natural history of the  
668 processionary moths (*Thaumetopoea* spp.): New insights in relation to climate change,  
669 in: Roques, A. (Ed.), *Processionary Moths and Climate Change : An Update*. Springer  
670 Netherlands, Dordrecht, pp. 15–79. [https://doi.org/10.1007/978-94-017-9340-7\\_2](https://doi.org/10.1007/978-94-017-9340-7_2)
- 671 Battisti, A., Larsson, S., Roques, A., 2017. Processionary moths and associated urtication risk:  
672 global change–driven effects. *Annual Review of Entomology* 62, 323–342.  
673 <https://doi.org/10.1146/annurev-ento-031616-034918>
- 674 Battisti, A., Stastny, M., Netherer, S., Robinet, C., Schopf, A., Roques, A., Larsson, S., 2005.  
675 Expansion of geographic range in the pine processionary moth caused by increased  
676 winter temperatures. *Ecological Applications* 15, 2084–2096.  
677 <https://doi.org/10.1890/04-1903>
- 678 Branco, M., Santos, M., Calvão, T., Telfer, G., Paiva, M.-R., 2008. Arthropod diversity  
679 sheltered in *Thaumetopoea pityocampa* (Lepidoptera: Notodontidae) larval nests:  
680 Arthropod diversity in larval nests. *Insect Conservation and Diversity* 1, 215–221.  
681 <https://doi.org/10.1111/j.1752-4598.2008.00028.x>
- 682 Breuer, M., Devkota, B., 1990. Studies on the importance of nest temperature of  
683 *Thaumetopoea pityocampa* (Den. & Schiff.) (Lep., Thaumetopoeidae). *Journal of*

684 Applied Entomology 109, 331–335. <https://doi.org/10.1111/j.1439->  
685 0418.1990.tb00060.x

686 Breuer, M., Devkota, B., Douma-Petridou, E., Koutsaftikis, A., Schmidt, G.H., 1989. Studies  
687 on the exposition and temperature of nests of *Thaumetopoea pityocampa* (Den. &  
688 Schiff.) (Lep., Thaumetopoeidae) in Greece. Journal of Applied Entomology 107,  
689 370–375. <https://doi.org/10.1111/j.1439-0418.1989.tb00271.x>

690 Cahon, T., Caillon, R., Pincebourde, S., 2018. Do aphids alter leaf surface temperature  
691 patterns during early infestation? Insects 9, 34. <https://doi.org/10.3390/insects9010034>

692 Caillon, R., Suppo, C., Casas, J., Woods, H.A., Pincebourde, S., 2014. Warming decreases  
693 thermal heterogeneity of leaf surfaces: implications for behavioural thermoregulation  
694 by arthropods. Functional Ecology 28, 1449–1458. <https://doi.org/10.1111/1365->  
695 2435.12288

696 Campbell, G.S., Norman, J.M., 1998. An introduction to environmental biophysics. Springer  
697 Verlag, New-York.

698 Carus, S., 2004. Impact of defoliation by the pine processionary moth (*Thaumetopoea*  
699 *pityocampa*) on radial, height and volume growth of calabrian pine (*Pinus brutia*) trees  
700 in Turkey. Phytoparasitica 32, 459–469. <https://doi.org/10.1007/BF02980440>

701 Chown, S.L., Nicolson, S.W., 2004. Insect physiological ecology: mechanisms and patterns.  
702 Oxford University Press, New York, USA.

703 Colacci, M., Kavallieratos, N.G., Athanassiou, C.G., Boukouvala, M.C., Rumbos, C.I.,  
704 Kontodimas, D.C., Pardo, D., Sancho, J., Benavent-Fernández, E., Gálvez-Settier, S.,  
705 Sciarretta, A., Trematerra, P., 2018. Management of the pine processionary moth,  
706 *Thaumetopoea pityocampa* (Lepidoptera: Thaumetopoeidae), in urban and suburban  
707 areas: trials with trunk barrier and adhesive barrier trap devices. Journal of Economic  
708 Entomology 111, 227–238. <https://doi.org/10.1093/jee/tox270>

709 Dawkins, R., 1982. The extended phenotype: the gene as the unit of selection. Oxford  
710 University Press 287.

711 de Boer, J., Harvey, J., 2020. Range-expansion in processionary moths and biological control.  
712 Insects 11, 267. <https://doi.org/10.3390/insects11050267>

713 Démolin, G., 1965. Grégairisme et subsocialité chez *Thaumetopoea pityocampa* Schiff. Nid  
714 d’hiver – activité de tissage. Compte Rendu du Ve congrès de l’union internationale  
715 pour l’étude des insectes sociaux. pp 69-77.

716 Fitzgerald, T.D., Miller, S., Smith, M., 2012. Thermal properties of the tent of early instar  
717 colonies of the eastern tent caterpillar, *Malacosoma americanum* (Lepidoptera:

718 Lasiocampidae). *Journal of Thermal Biology* 37, 615–624.  
719 <https://doi.org/10.1016/j.jtherbio.2012.07.010>

720 Gates, D., Schmerl, R.B., 1980. *Perspectives of biophysical ecology*. Springer-Verlag.  
721 Hansell, M., 2007. *Built by animals: the natural history of animal architecture*. Oxford  
722 University Press, New York, USA.

723 Heinrich, B., 1999. *The thermal warriors: strategies of insect survival*. Harvard University  
724 Press, Cambridge, Massachusetts, USA.

725 Hódar, J.A., Castro, J., Zamora, R., 2003. Pine processionary caterpillar *Thaumetopoea*  
726 *pityocampa* as a new threat for relict Mediterranean Scots pine forests under climatic  
727 warming. *Biological Conservation* 110, 123–129. [https://doi.org/10.1016/S0006-](https://doi.org/10.1016/S0006-3207(02)00183-0)  
728 [3207\(02\)00183-0](https://doi.org/10.1016/S0006-3207(02)00183-0)

729 Hozumi, S., Mateus, S., Kudô, K., Kuwahara, T., Yamane, S., Zucchi, R., 2010. Nest  
730 thermoregulation in *Polybia scutellaris* (White) (Hymenoptera: Vespidae).  
731 *Neotropical Entomology* 39, 826–828. [https://doi.org/10.1590/S1519-](https://doi.org/10.1590/S1519-566X2010000500024)  
732 [566X2010000500024](https://doi.org/10.1590/S1519-566X2010000500024)

733 Huchon, H., Demolin, G., 1970. La bioécologie de la Processionnaire du pin : dispersion  
734 potentielle, dispersion actuelle. *Revue Forestière Française* 220.  
735 <https://doi.org/10.4267/2042/20421>

736 IPCC, 2015. *Changements climatiques 2014: rapport de synthèse : contribution des Groupes*  
737 *de travail I, II et III au cinquième Rapport d'évaluation du Groupe d'experts*  
738 *intergouvernemental sur l'évolution du climat*. GIEC, Genève (Suisse).

739 Jactel, H., Barbaro, L., Battisti, A., Bosc, A., Branco, M., Brockerhoff, E., Castagneyrol, B.,  
740 Dulaurent, A.-M., Hódar, J.A., Jacquet, J.-S., Mateus, E., Paiva, M.-R., Roques, A.,  
741 Samalens, J.-C., Santos, H., Schlyter, F., 2015. Insect – tree interactions in  
742 *Thaumetopoea pityocampa*, in: Roques, A. (Ed.), *Processionary Moths and Climate*  
743 *Change : An Update*. Springer Netherlands, Dordrecht, pp. 265–310.  
744 [https://doi.org/10.1007/978-94-017-9340-7\\_6](https://doi.org/10.1007/978-94-017-9340-7_6)

745 Joos, B., Casey, T.M., Fitzgerald, T.D., Buttemer, W.A., 1988. Roles of the tent in behavioral  
746 thermoregulation of eastern tent caterpillars. *Ecology* 69, 2004–2011.  
747 <https://doi.org/10.2307/1941178>

748 Joseph, G.S., Seymour, C.L., Coetzee, B.W.T., Ndlovu, M., De La Torre, A., Suttle, R.,  
749 Hicks, N., Oxley, S., Foord, S.H., 2016. Microclimates mitigate against hot  
750 temperatures in dryland ecosystems: termite mounds as an example. *Ecosphere* 7.  
751 <https://doi.org/10.1002/ecs2.1509>

752 Kaspari, M., Clay, N.A., Lucas, J., Yanoviak, S.P., Kay, A., 2015. Thermal adaptation  
753 generates a diversity of thermal limits in a rainforest ant community. *Global Change*  
754 *Biology* 21, 1092–102. <https://doi.org/10.1111/gcb.12750>

755 Kearney, M., Porter, W., 2009. Mechanistic niche modelling: combining physiological and  
756 spatial data to predict species' ranges. *Ecology Letters* 12, 334–350.  
757 <https://doi.org/10.1111/j.1461-0248.2008.01277.x>

758 Knapp, R., Casey, T.M., 1986. Thermal ecology, behavior, and growth of gypsy moth and  
759 eastern tent caterpillars. *Ecology* 67, 598–608. <https://doi.org/10.2307/1937683>

760 Kührt, U., Samietz, J., Dorn, S., 2005. Thermoregulation behaviour in codling moth larvae.  
761 *Physiological Entomology* 30, 54–61. <https://doi.org/10.1111/j.0307->  
762 [6962.2005.00431.x](https://doi.org/10.1111/j.0307-6962.2005.00431.x)

763 L. Monteith, J., E. Reifsnyder, W., 2008. *Principles of environmental physics*, 3rd Edition. ed.  
764 Elsevier. <https://doi.org/10.1063/1.3128494>

765 Lembrechts, J.J., Aalto, J., Ashcroft, M.B., De Frenne, P., Kopecký, M., Lenoir, J., Luoto, M.,  
766 Maclean, I.M.D., Rouspard, O., Fuentes-Lillo, E., García, R.A., Pellissier, L.,  
767 Pitteloud, C., Alatalo, J.M., Smith, S.W., Björk, R.G., Muffler, L., Cesarz, S.,  
768 Gottschall, F., Backes, A.R., Okello, J., Urban, J., Plichta, R., Svátek, M., Phartyal,  
769 S.S., Wipf, S., Eisenhauer, N., Puşcaş, M., Dan Turtureanu, P., Varlagin, A., Dimarco,  
770 R.D., Jump, A.S., Randall, K., Dorrepaal, E., Larson, K., Walz, J., Vitale, L.,  
771 Svoboda, M., Finger Higgins, R., Halbritter, A.H., Curasi, S.R., Klupar, I., Koontz,  
772 A., Pearse, W.D., Simpson, E., Stemkovski, M., Graae, B.J., Vedel Sørensen, M.,  
773 Høye, T.T., Fernández Calzado, M.R., Lorite, J., Carbognani, M., Tomaselli, M.,  
774 Forte, T.G.W., Petraglia, A., Haesen, S., Somers, B., Van Meerbeek, K., Björkman,  
775 M.P., Hylander, K., Merinero, S., Gharun, M., Buchmann, N., Dolezal, J., Matula, R.,  
776 Thomas, A.D., Bailey, J.J., Ghosn, D., Kazakis, G., de Pablo, M.A., Kemppinen, J.,  
777 Niittynen, P., Rew, L., Seipel, T., Larson, C., Speed, J.D.M., Ardö, J., Cannone, N.,  
778 Guglielmin, M., Malfasi, F., Bader, M.Y., Canessa, R., Stanisci, A., Kreyling, J.,  
779 Schmeddes, J., Teuber, L., Aschero, V., Čiliak, M., Máliš, F., De Smedt, P., Govaert,  
780 S., Meeussen, C., Vangansbeke, P., Gigauri, K., Lamprecht, A., Pauli, H., Steinbauer,  
781 K., Winkler, M., Ueyama, M., Nuñez, M.A., Ursu, T.-M., Haider, S., Wedegärtner,  
782 R.E.M., Smiljanic, M., Trouillier, M., Wilmking, M., Altman, J., Brúna, J., Hederová,  
783 L., Macek, M., Man, M., Wild, J., Vittoz, P., Pärtel, M., Barančok, P., Kanka, R.,  
784 Kollár, J., Palaj, A., Barros, A., Mazzolari, A.C., Bauters, M., Boeckx, P., Benito  
785 Alonso, J.L., Zong, S., Di Cecco, V., Sitková, Z., Tielbörger, K., van den Brink, L.,

786 Weigel, R., Homeier, J., Dahlberg, C.J., Medinets, S., Medinets, V., De Boeck, H.J.,  
787 Portillo-Estrada, M., Verryck, L.T., Milbau, A., Daskalova, G.N., Thomas, H.J.D.,  
788 Myers-Smith, I.H., Blonder, B., Stephan, J.G., Descombes, P., Zellweger, F., Frei,  
789 E.R., Heinesch, B., Andrews, C., Dick, J., Siebicke, L., Rocha, A., Senior, R.A.,  
790 Rixen, C., Jimenez, J.J., Boike, J., Pauchard, A., Scholten, T., Scheffers, B., Klinges,  
791 D., Basham, E.W., Zhang, J., Zhang, Z., Géron, C., Fazlioglu, F., Candan, O., Sallo  
792 Bravo, J., Hrbacek, F., Laska, K., Cremonese, E., Haase, P., Moyano, F.E., Rossi, C.,  
793 Nijs, I., 2020. SoilTemp: a global database of near-surface temperature. *Global*  
794 *Change Biology* 26, 6616–6629. <https://doi.org/10.1111/gcb.15123>

795 Martin, J.-C., 2005. La processionnaire du pin *Thaumetopoea pityocampa*, biologie et  
796 protection des forêts. INRA.

797 May, M.L., 1979. Insect thermoregulation. *Annual Review of Entomology* 24, 313–349.  
798 <https://doi.org/10.1146/annurev.en.24.010179.001525>

799 Menéndez, R., 2007. How are insects responding to global warming? *Tijdschrift voor*  
800 *Entomologie* 150, 12.

801 Moneo, I., Battisti, A., Dufour, B., García-Ortiz, J., González-Muñoz, M., Moutou, F.,  
802 Paolucci, P., Petrucco Toffolo, E., Rivière, J., Rodríguez-Mahillo, A.-I., Roques, A.,  
803 Roques, L., Vega, Jose, Vega, Jackeline, 2015. Medical and veterinary impact of the  
804 urticating processionary larvae. *Processionary Moths and Climate Change: An Update*  
805 359–410. [https://doi.org/10.1007/978-94-017-9340-7\\_8](https://doi.org/10.1007/978-94-017-9340-7_8)

806 Parlak, S., Özçankaya, İ.M., Batur, M., Akkaş, M.E., Boza, Z., Toprak, Ö., 2019. Determining  
807 the edge effect of pine processionary moth (*Thaumetopoea pityocampa*) in its  
808 horizontal distribution in the stand. *Journal of Forest Research* 30, 347–352.  
809 <https://doi.org/10.1007/s11676-018-0634-5>

810 Pike, D. a., Webb, J.K., Shine, R., 2012. Hot mothers, cool eggs: nest-site selection by egg-  
811 guarding spiders accommodates conflicting thermal optima. *Functional Ecology* 26,  
812 469–475. <https://doi.org/10.1111/j.1365-2435.2011.01946.x>

813 Pimentel, C., Ferreira, C., Nilsson, J.-Å., 2010. Latitudinal gradients and the shaping of life-  
814 history traits in a gregarious caterpillar. *Biological Journal of the Linnean Society* 100,  
815 224–236. <https://doi.org/10.1111/j.1095-8312.2010.01413.x>

816 Pincebourde, S., Casas, J., 2016. Hypoxia and hypercarbia in endophagous insects: Larval  
817 position in the plant gas exchange network is key. *Journal of Insect Physiology* 84,  
818 137–153. <https://doi.org/10.1016/j.jinsphys.2015.07.006>

819 Pincebourde, S., Casas, J., 2015. Warming tolerance across insect ontogeny: influence of joint  
820 shifts in microclimates and thermal limits. *Ecology* 96, 986–997.  
821 <https://doi.org/10.1890/14-0744.1>

822 Pincebourde, S., Casas, J., 2006. Multitrophic biophysical budgets: Thermal ecology of an  
823 intimate herbivore insect-plant interaction. *Ecological Monographs* 76, 175–194.  
824 [https://doi.org/10.1890/0012-9615\(2006\)076\[0175:MBBTEO\]2.0.CO;2](https://doi.org/10.1890/0012-9615(2006)076[0175:MBBTEO]2.0.CO;2)

825 Pincebourde, S., Murdock, C.C., Vickers, M., Sears, M.W., 2016. Fine-scale microclimatic  
826 variation can shape the responses of organisms to global change in both natural and  
827 urban environments. *Integrative and Comparative Biology* 56, 45–61.  
828 <https://doi.org/10.1093/icb/icw016>

829 Pincebourde, S., Sallé, A., 2020. On the importance of getting fine-scale temperature records  
830 near any surface. *Global Change Biology* 26, 6025– 6027.

831 Pincebourde, S., Sinoquet, H., Combes, D., Casas, J., 2007. Regional climate modulates the  
832 canopy mosaic of favourable and risky microclimates for insects. *Journal of Animal*  
833 *Ecology* 76, 424–438. <https://doi.org/10.1111/j.1365-2656.2007.01231.x>

834 Pincebourde, S., Woods, H.A., 2020. There is plenty of room at the bottom: microclimates  
835 drive insect vulnerability to climate change. *Current Opinion in Insect Science* 41, 63–  
836 70. <https://doi.org/10.1016/j.cois.2020.07.001>

837 Potter, K.A., Woods, H.A., Pincebourde, S., 2013. Microclimatic challenges in global change  
838 biology. *Global Change Biology* 19, 2932–2939. <https://doi.org/10.1111/gcb.12257>

839 R Core Team (2018). R: A language and environment for statistical computing. R Foundation  
840 for Statistical Computing, Vienna, Austria. Available online at [https://www.R-](https://www.R-project.org/)  
841 [project.org/.](https://www.R-project.org/), n.d.

842 Rehnberg, B.G., 2002. Heat retention by webs of the fall webworm *Hyphantria cunea*  
843 (Lepidoptera: Arctiidae): infrared warming and forced convective cooling. *Journal of*  
844 *Thermal Biology* 27, 525–530. [https://doi.org/10.1016/S0306-4565\(02\)00026-8](https://doi.org/10.1016/S0306-4565(02)00026-8)

845 Robinet, C., Baier, P., Pennerstorfer, J., Schopf, A., Roques, A., 2007. Modelling the effects  
846 of climate change on the potential feeding activity of *Thaumetopoea pityocampa* (Den.  
847 & Schiff.) (Lep., Notodontidae) in France. *Global Ecology and Biogeography* 16,  
848 460–471. <https://doi.org/10.1111/j.1466-8238.2006.00302.x>

849 Ronnås, C., Larsson, S., Pitacco, A., Battisti, A., 2010. Effects of colony size on larval  
850 performance in a processionary moth. *Ecological Entomology* 35, 436–445.  
851 <https://doi.org/10.1111/j.1365-2311.2010.01199.x>

852 Roques, A., 2015. Processionary moths and climate change: an update. Springer, New York.

853 Ruf, C., Fiedler, K., 2002a. Tent-based thermoregulation in social caterpillars of *Eriogaster*  
854 *lanestris* (Lepidoptera: Lasiocampidae): behavioral mechanisms and physical features  
855 of the tent. *Journal of Thermal Biology* 27, 493–501. [https://doi.org/10.1016/S0306-](https://doi.org/10.1016/S0306-4565(02)00022-0)  
856 [4565\(02\)00022-0](https://doi.org/10.1016/S0306-4565(02)00022-0)

857 Ruf, C., Fiedler, K., 2000b. Thermal gains through collective metabolic heat production in  
858 social caterpillars of *Eriogaster lanestris*. *Naturwissenschaften* 87, 193–196.  
859 <https://doi.org/10.1007/s001140050702>

860 Samalens, J.-C., Rossi, J.-P., 2011. Does landscape composition alter the spatiotemporal  
861 distribution of the pine processionary moth in a pine plantation forest? *Population*  
862 *Ecology* 53, 287–296. <https://doi.org/10.1007/s10144-010-0227-4>

863 Santos, H., Rousset, J., Magnoux, E., Paiva, M.-R., Branco, M., Kerdelhué, C., 2007.  
864 Genetic isolation through time: allochronic differentiation of a phenologically atypical  
865 population of the pine processionary moth. *Proceedings of the Royal Society B:*  
866 *Biological Sciences* 274, 935–941. <https://doi.org/10.1098/rspb.2006.3767>

867 Saudreau, M., Ezanic, A., Adam, B., Caillon, R., Walser, P., Pincebourde, S., 2017.  
868 Temperature heterogeneity over leaf surfaces: the contribution of the lamina  
869 microtopography. *Plant Cell and Environment* 40, 2174–2188.  
870 <https://doi.org/10.1111/pce.13026>

871 Saudreau, M., Marquier, A., Adam, B., Monney, P., Sinoqueta, H., 2009. Experimental study  
872 of fruit temperature dynamics within apple tree crowns. *Agricultural and Forest*  
873 *Meteorology* 149, 362–372. <https://doi.org/10.1016/j.agrformet.2008.09.001>

874 Sinclair, B.J., Marshall, K.E., Sewell, M.A., Levesque, D.L., Willett, C.S., Slotsbo, S., Dong,  
875 Y., Harley, C.D.G., Marshall, D.J., Helmuth, B.S., Huey, R.B., 2016. Can we predict  
876 ectotherm responses to climate change using thermal performance curves and body  
877 temperatures? *Ecology Letters* 19, 1372–1385. <https://doi.org/10.1111/ele.12686>

878 Stabentheiner, A., Kovac, H., Brodschneider, R., 2010. Honeybee colony thermoregulation –  
879 regulatory mechanisms and contribution of individuals in dependence on age, location  
880 and thermal stress. *PLoS ONE* 5, e8967. <https://doi.org/10.1371/journal.pone.0008967>

881 Walther, G.-R., Post, E., Convey, P., Menzel, A., Parmesan, C., Beebee, T.J.C., Fromentin, J.-  
882 M., Hoegh-Guldberg, O., Bairlein, F., 2002. Ecological responses to recent climate  
883 change. *Nature* 416, 389–395. <https://doi.org/10.1038/416389a>

884 Willmer, P.G., 1982. Microclimate and the environmental physiology of insects, in: *Advances*  
885 *in Insect Physiology*. Elsevier, pp. 1–57. [https://doi.org/10.1016/S0065-](https://doi.org/10.1016/S0065-2806(08)60151-4)  
886 [2806\(08\)60151-4](https://doi.org/10.1016/S0065-2806(08)60151-4)



887 Woods, H.A., Dillon, M.E., Pincebourde, S., 2015. The roles of microclimatic diversity and of  
888 behavior in mediating the responses of ectotherms to climate change. *Journal of*  
889 *Thermal Biology* 54, 86–97. <https://doi.org/10.1016/j.jtherbio.2014.10.002>  
890